Gas-Phase Enantioselectivity of Chiral *N*-Linked Peptidoresorc[4]arene Isomers toward Dipeptides†

Bruno Botta,* Caterina Fraschetti, Ilaria D'Acquarica, and Maurizio Speranza*

Dipartimento di Chimica e Tecnologie del Farmaco, "Sapienza" Università di Roma, P.le Aldo Moro 5, 00185 Roma, Italy

Francesca R. Novara

Institut für Chemie der Technischen Universität Berlin, Strasse des 17. Juni 135, 10623 Berlin, Germany

Jochen Mattay and Matthias C. Letzel

Fakultät für Chemie, Universität Bielefeld, Postfach 100131, 33501 Bielefeld, Germany

Received: May 11, 2009; Revised Manuscript Received: June 15, 2009

The gas-phase enantioselectivity of cone *N*-linked peptidoresorc[4]arenes (generally symbolized as M) toward the homologue dipeptides (generally symbolized as A) has been evaluated by measuring the kinetics of the A release from the diastereomeric $[M \cdot H \cdot A]^+$ complexes induced by (*R*)-(−)-2-butylamine (B). In most cases investigated, the heterochiral $[M \cdot H \cdot A]^+$ complexes, namely those wherein the configuration of the A guest is opposite to that of the host M pendants, react faster (up to 5 times) than the homochiral analogues, wherein guest A guest has the same configuration of the host M pendants. The kinetic results, discussed in the light of previous MS and NMR evidence, indicate that both the efficiency and the enantioselectivity of the guest exchange reaction depend essentially on the structure and the relative stability of the diastereomeric $[M \cdot H \cdot A]^+$ complexes. These, in turn, depend on the functional groups and the configuration of both the guest and the host pendants. The absence of any significant effects of the B configuration indicates that, in all systems investigated, the dipeptide guest A is predominantly located outside the host chiral cavity.

Introduction

Enzymes are proteic biopolymers endowed with cavities of appropriate shape and size holding suitable functionalities in specific positions. A key supramolecular feature of enzymes is their capability of "molecular recognition". According to this property, the binding and insertion into the active site of a particular biomolecule is extremely selective and is based on the ability of the enzyme to recognize the guest by its size, shape, and chemical features.[1−4] A significant role is also played by the extensive desolvation of the guest molecule entering the receptor cavity which not only favors its uptake but also greatly enhances its reactivity.[5]

The amazing properties of enzymes motivate chemists for the design of "synthetic enzymes" as exemplars for understanding the mechanism of action of enzymes and for attempting to reproduce them for practical applications. Among various molecular platforms that can be proposed for the construction of artificial receptors, macrocycles of multiple aromatic units have widely been used. An important step toward the elucidation of enzyme mechanisms requires a comprehensive kinetic study on simplified models under conditions, like the gas phase, where the noncovalent interactions in the guest/host complex are not perturbed by medium effects.[6]

An important family of aromatic macrocycles, often employed as building blocks in molecular recognition, are calixarenes.[7] They are important cavity-forming modules and have been exploited for the preparation of cavitands,[8] (hemi)carcerands,[9] and self-assembling capsules.[10] Among them, only a few examples of resorcarenes equipped with *N*- linked dipeptide residues at the feet are known from the literature. In previous studies, resorc[4]arene octamethyl ethers have been functionalized at the feet with L- and D-valine ethyl ester units,[11] and their capability of selectively encapsulating chiral amino acids has been investigated in the gas phase by mass spectrometry (MS)[12] as well as in solution by NMR spectroscopy.[13] Later on, the same methodologies have been employed to functionalize at the feet resorc[4]arene octamethyl ethers with leucyl−valine (LL-($\mathbf{I}_L$); DD-($\mathbf{I}_D$); Chart 1) and valyl−leucine (LL-($\mathbf{III}_L$); DD-($\mathbf{III}_D$); Chart 1; see Supporting Information) methyl esters and to investigate their affinity toward the same dipeptide esters used in their synthesis, namely, leucyl−valine−OMe (LL-($\mathbf{1}_L$); DD-($\mathbf{1}_D$); Chart 1) and valyl−leucine−OMe (LL-($\mathbf{3}_L$); DD-($\mathbf{3}_D$); Chart 1).[14] It was found that macrocycles **I** and **III** (henceforth symbolized as M) are capable of selectively encapsulating the homologue dipeptides **1** and **3** (henceforth symbolized as A), respectively, both in solution and in the gas phase, and of forming relatively stable host/guest $[M \cdot A]$ complexes resistant to chromatographic purification but not to heating. On the grounds of NMR DOSY evidence, the homochiral $[\mathbf{I}_L \cdot \mathbf{1}_L]$ complex was appreciably more stable than the heterochiral $[\mathbf{I}_L \cdot \mathbf{1}_D]$ one, at least in $CDCl_3$ at room temperature. Finally, NMR 1D ROESY experiments suggested that the interaction between the resorcarene host and the dipeptide guest in $[\mathbf{I}_L \cdot \mathbf{1}_L]$ mainly occurs at the external surface of the host by means of attractive hydrogen bonding among the polar groups of the A and the M pendants. Along this line, we focus our attention on measuring the gas-phase enantioselectivity of the reaction between proton-bound diastereomeric $[M \cdot H \cdot A]^+$ (M = **I**−**IV**; A = **1**−**3**)

† Part of the "Vincenzo Aquilanti Festschrift".

10.1021/jp904374h
Published on Web 07/09/2009

CHART 1: Formulas of 2,8,14,20-Tetrakis(leucyl-valinamido)resorc[4]arene Methyl ($I_{D/L}$) and Ethyl Tetra-ester (II_L); 2,8,14,20-Tetrakis(valyl-leucinamido)resorc[4]arene Ethyl Tetra-ester ($III_{D/L}$) and Tetra-acid ($IV_{D/L}$)) and of Leucyl−Valine−OMe ($1_{D/L}$), L-Leucyl−L-Valine−OEt (2_L), and Valyl−Leucine−OMe ($3_{D/L}$)[a]

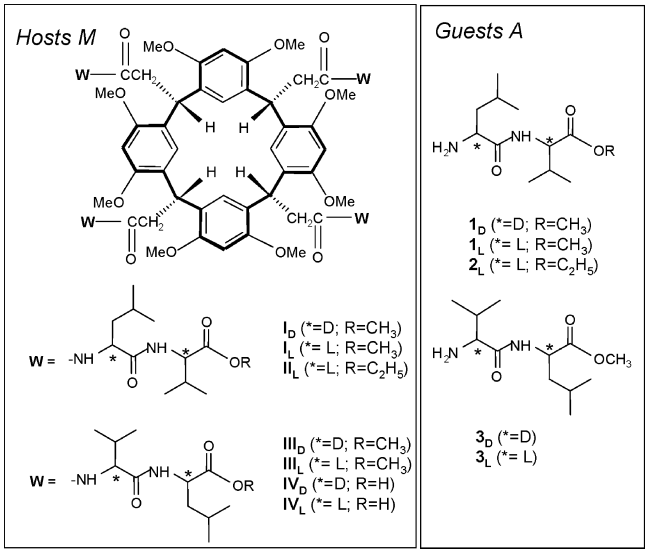

[a] The asterisks denote the chiral centers, either LL or DD.

complexes toward (*R*)-(−)-2-butylamine (B) (eqs 1a and 1b). The aim of this study is to shed some light on the specific M/A interactions in $[M\cdot H\cdot A]^+$ through (a) the measure of the effects of both the guest A and the host M configuration on the reaction enantioselectivity, (b) the measure of the effects of the amino acid sequencing in the dipeptide esters as well as in the dipeptidic pendants of the hosts M, and (c) the measure of the effects of the −COOR function (R = H, CH_3, C_2H_5) in the guest A and the host M pendants.

$$[M_L\cdot H\cdot A_L]^+ \xrightarrow[+B\ -\ A_L]{k^{LL}} [M_L\cdot H\cdot B]^+ \xleftarrow[+B\ -\ A_D]{k^{LD}} [M_L\cdot H\cdot A_D]^+ \quad (1a)$$

$$[M_D\cdot H\cdot A_L]^+ \xrightarrow[+B\ -\ A_L]{k^{DL}} [M_D\cdot H\cdot B]^+ \xleftarrow[+B\ -\ A_D]{k^{DD}} [M_D\cdot H\cdot A_D]^+ \quad (1b)$$

Results and Discussion

The proton-bonded two-body complexes $[M\cdot H\cdot A]^+$ have been generated by electrospray ionization (ESI) into a Fourier transform ion cyclotron resonance mass spectrometer (FT-ICR-MS) and allowed to react with B, present in the FT-ICR-MS cell at fixed concentrations. The formation of the reaction product $[M\cdot H\cdot B]^+$ was monitored as a function of time *t*. If *I* is the intensity of complex $[M\cdot H\cdot A]^+$ at the delay time *t* and I_0 is the sum of the intensities of $[M\cdot H\cdot A]^+$ and $[M\cdot H\cdot B]^+$, linear $\ln(I/I_0)$ vs *t* plots were invariably observed in the reaction of amine B with all the $[M\cdot H\cdot A]^+$ (M = **I**−**III**) complexes (correlation coefficient $0.984 < r^2 < 0.999$) (Figure 1). Their exceedingly good linearity indicates that a single $[M\cdot H\cdot A]^+$ (M = **I**−**III**) structure is predominantly formed and thermalized by multiple unreactive collisions with argon before reacting with B.

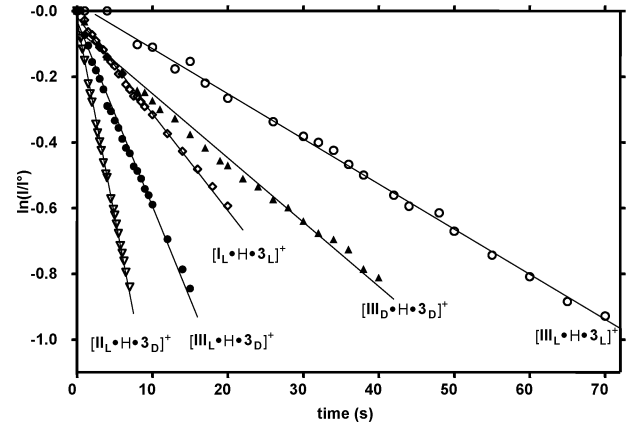

Figure 1. Typical monoexponential kinetics of some representative $[M\cdot H\cdot A]^+$ (M = **I**−**III**) complexes. Other systems with M = **I**−**III** not included in the figure behave similarly.

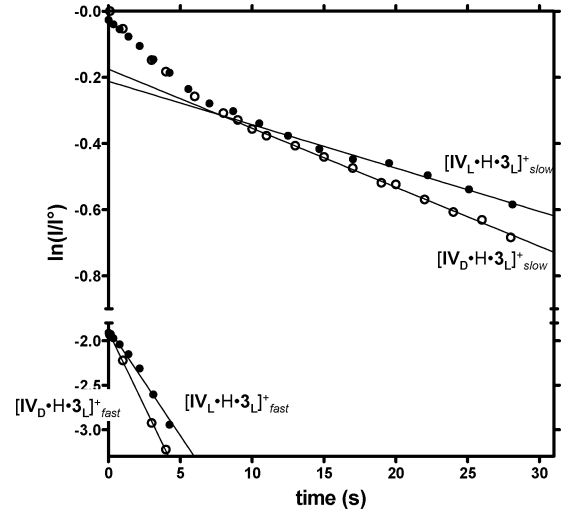

Figure 2. Typical biexponential kinetics of some representative $[\mathbf{IV}\cdot H\cdot A]^+$ complexes. Other systems with M = **IV** not included in the figure behave similarly.

In contrast, biexponential kinetics are observed with $[\mathbf{IV}\cdot H\cdot A]^+$ (Figure 2). As pointed out in related studies,[12] this kinetic behavior is ascribed to the occurrence of two stable isomeric $[\mathbf{IV}\cdot H\cdot A]^+$ structures, one less reactive ($[\mathbf{IV}\cdot H\cdot A]^+_{slow}$) and the other more reactive ($[\mathbf{IV}\cdot H\cdot A]^+_{fast}$). The time dependence of $[\mathbf{IV}\cdot H\cdot A]^+_{fast}$ (correlation coefficient $0.983 < r^2 < 0.999$) (lines at the bottom of Figure 2) can be inferred from the overall $[\mathbf{IV}\cdot H\cdot A]^+$ decay after subtracting the first-order decay of $[\mathbf{IV}\cdot H\cdot A]^+_{slow}$ (correlation coefficient $0.988 < r^2 < 0.997$) (lines at the top of Figure 2). The two isomeric structures react with the amine B at rates differing by a factor of ca. 20. The *Y*-intercepts of the first-order decay of $[\mathbf{IV}\cdot H\cdot A]^+_{slow}$ and $[\mathbf{IV}\cdot H\cdot A]^+_{fast}$ provide an estimate of their relative distribution.

The pseudo-first-order rate constants k' of eqs 1a and 1b were obtained from the slopes of the relevant $\ln(I/I_0)$ vs *t* plots. The corresponding second-order rate constants *k* are calculated from the ratio between the slope of the first-order plots and the concentration of B. Their values, compared with the relevant collision rate constants (k_{coll}), estimated according to Su's trajectory calculation method,[15] provides the efficiency of the reaction (eff = $100k/k_{coll}$) (figures in parentheses in Table 1).

The reaction enantioselectivity is defined by the $\gamma^D = k^{DD}/k^{DL}$ and $\gamma^L = k^{LL}/k^{LD}$ ratios, which provide a measure of the effect of the guest A configuration relative to that of the host M

TABLE 1: Configurational Effects on Reaction Kinetics[a]

guest (A)		host	host configuration: D	host configuration: L
$\mathbf{1}_D$		**I**	$k^{DD} = 1.70 \pm 0.13$ (1.5)	$k^{LD} = 4.76 \pm 0.29$ (4.1)
$\mathbf{1}_L$			$k^{DL} = 3.88 \pm 0.18$ (3.3)	$k^{LL} = 1.50 \pm 0.12$ (1.3)
$\mathbf{1}_D$		**III**	$k^{DD} = 0.88 \pm 0.07$ (0.8)	$k^{LD} = 3.09 \pm 0.23$ (2.7)
$\mathbf{1}_L$			$k^{DL} = 2.86 \pm 0.16$ (2.6)	$k^{LL} = 0.73 \pm 0.06$ (0.6)
$\mathbf{1}_D$	fast	**IV**	$k^{DD} = 1.46 \pm 0.16$ (1.2)	$k^{LD} = 1.29 \pm 0.15$ (1.1)
$\mathbf{1}_L$	fast		$k^{DL} = 1.48 \pm 0.16$ (1.3)	$k^{LL} = 1.18 \pm 0.13$ (1.0)
$\mathbf{1}_D$	slow	**IV**	$k^{DD} = 0.08 \pm 0.01$ (0.1)	$k^{LD} = 0.08 \pm 0.01$ (0.1)
$\mathbf{1}_L$	slow		$k^{DL} = 0.09 \pm 0.01$ (0.1)	$k^{LL} = 0.07 \pm 0.01$ (0.1)
$\mathbf{3}_D$		**I**	$k^{DD} = 2.83 \pm 0.16$ (2.4)	$k^{LD} = 4.96 \pm 0.21$ (4.3)
$\mathbf{3}_L$			$k^{DL} = 3.76 \pm 0.18$ (3.2)	$k^{LL} = 2.49 \pm 0.13$ (2.1)
$\mathbf{3}_D$		**III**	$k^{DD} = 1.47 \pm 0.10$ (1.3)	$k^{LD} = 4.95 \pm 0.33$ (4.3)
$\mathbf{3}_L$			$k^{DL} = 4.09 \pm 0.27$ (3.5)	$k^{LL} = 1.03 \pm 0.09$ (0.9)
$\mathbf{3}_D$	fast	**IV**	$k^{DD} = 1.31 \pm 0.14$ (1.1)	$k^{LD} = 1.25 \pm 0.14$ (1.1)
$\mathbf{3}_L$	fast		$k^{DL} = 1.44 \pm 0.15$ (1.2)	$k^{LL} = 1.32 \pm 0.14$ (1.1)
$\mathbf{3}_D$	slow	**IV**	$k^{DD} = 0.14 \pm 0.01$ (0.1)	$k^{LD} = 0.07 \pm 0.01$ (0.1)
$\mathbf{3}_L$	slow		$k^{DL} = 0.07 \pm 0.01$ (0.1)	$k^{LL} = 0.12 \pm 0.01$ (0.1)
$\mathbf{1}_D$		**II**		$k^{LD} = 5.41 \pm 0.32$ (4.7)
$\mathbf{1}_L$				$k^{LL} = 1.76 \pm 0.13$ (1.5)
$\mathbf{2}_L$		**I**	$k^{DL} = 2.13 \pm 0.14$ (1.8)	$k^{LL} = 0.96 \pm 0.07$ (0.8)
$\mathbf{2}_L$		**II**		$k^{LL} = 1.45 \pm 0.12$ (0.8)
$\mathbf{2}_L$		**III**		$k^{LL} = 0.35 \pm 0.04$ (0.3)
$\mathbf{3}_L$		**II**		$k^{LL} = 3.82 \pm 0.19$ (3.3)

[a] $10^{11}k$ cm^3 molecule^{-1} s^{-1}; reaction efficiency in parentheses (eff $= 100 \times k/k_{coll}$, with the collision constant k_{coll} as calculated according to ref 15).

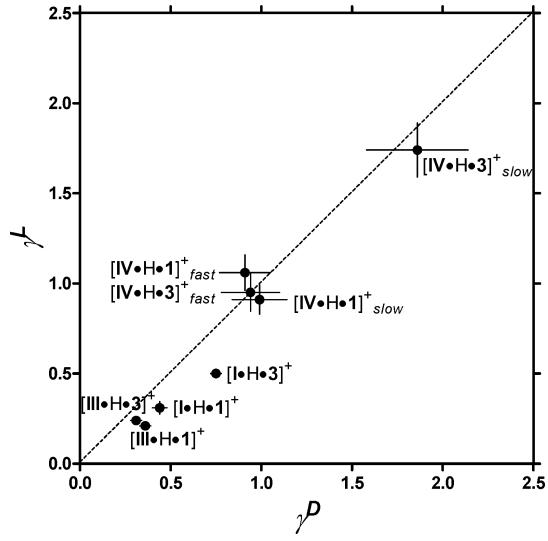

Figure 3. Reaction enantioselectivity: γ^L vs γ^D correlation.

pendants (Figure 3). The closeness of the γ^L vs γ^D points of Figure 3 to the broken line of unity slope ($\gamma^L = \gamma^D$) suggests that the B configuration plays no appreciable role in the reaction 1a and 1b kinetics. According to Figure 3, the heterochiral $[M \cdot H \cdot A]^+$ (M = **I**−**III**) complexes are more reactive than their homochiral counterparts, as witnessed by the relevant γ factors which invariably fall well below unity ($0.31 \pm 0.03 < \gamma^D < 0.75 \pm 0.03$; $0.21 \pm 0.02 < \gamma^L < 0.50 \pm 0.02$). In contrast, the slow components of the heterochiral $[\mathbf{IV} \cdot H \cdot \mathbf{3}]^+$ complexes appear less reactive than their homochiral counterparts ($\gamma^D = 1.86 \pm 0.28$; $\gamma^L = 1.74 \pm 0.26$), while their fast isomers are equally reactive ($\gamma^D \approx 1$; $\gamma^L \approx 1$). Finally, both the fast and the slow components of the diastereomeric $[\mathbf{IV} \cdot H \cdot \mathbf{1}]^+$ pair show no significant enantioselectivity ($\gamma^D \approx 1$; $\gamma^L \approx 1$).

The effect of estereal function (COOMe vs COOEt) of the dipeptidic guest on the reaction kinetics is expressed by the rate constant ratios ε^G of Table 2. The ε^H factors of Table 3 instead provide a measure of the effect of the COOR (R = H, CH_3, or C_2H_5) functionality of the host pendants. The rate constant ratios

TABLE 2: Effects of the −COOR Group of the Guest (ε^G)

guest (I) leu-valOMe	guest (II) leu-valOEt	host (M)	$\varepsilon^G = (k^{XY}([M \cdot H \cdot \text{Guest (I)}]^+))/(k^{XY}([M \cdot H \cdot \text{Guest (II)}]^+))$
$\mathbf{1}_L$	$\mathbf{2}_L$	$\mathbf{I}_L$	1.56 ± 0.17
$\mathbf{1}_L$	$\mathbf{2}_L$	$\mathbf{I}_D$	1.82 ± 0.16
$\mathbf{1}_L$	$\mathbf{2}_L$	$\mathbf{II}_L$	1.21 ± 0.13
$\mathbf{1}_L$	$\mathbf{2}_L$	$\mathbf{III}_D$	1.78 ± 0.17
$\mathbf{1}_L$	$\mathbf{2}_L$	$\mathbf{III}_L$	2.09 ± 0.28

TABLE 3: Effects of the −COOR Group of the Host Pendants (ε^H)

guest A	host (I)	host (II)		$\varepsilon^H = (k^{XY}([\text{Host (I)} \cdot H \cdot A]^+))/(k^{XY}([\text{Host (II)} \cdot H \cdot A]^+))$
	R = CH_3	R = C_2H_5		
$\mathbf{1}_D$	$\mathbf{I}_L$	$\mathbf{II}_L$		0.88 ± 0.07
$\mathbf{1}_L$	$\mathbf{I}_L$	$\mathbf{II}_L$		0.85 ± 0.09
	R = CH_3	R = H		
$\mathbf{1}_D$	$\mathbf{III}_L$	$\mathbf{IV}_L$	fast	2.39 ± 0.33
			slow	39.6 ± 5.9
$\mathbf{1}_L$	$\mathbf{III}_L$	$\mathbf{IV}_L$	fast	0.62 ± 0.08
			slow	9.86 ± 1.56
$\mathbf{1}_L$	$\mathbf{III}_D$	$\mathbf{IV}_D$	fast	1.93 ± 0.25
			slow	32.5 ± 4.1
$\mathbf{1}_D$	$\mathbf{III}_D$	$\mathbf{IV}_D$	fast	0.60 ± 0.08
			slow	10.6 ± 1.5
$\mathbf{3}_D$	$\mathbf{III}_L$	$\mathbf{IV}_L$	fast	3.96 ± 0.52
			slow	71.7 ± 11.4
$\mathbf{3}_L$	$\mathbf{III}_L$	$\mathbf{IV}_L$	fast	0.78 ± 0.11
			slow	8.58 ± 1.04
$\mathbf{3}_L$	$\mathbf{III}_D$	$\mathbf{IV}_D$	fast	2.84 ± 0.35
			slow	55.3 ± 8.3
$\mathbf{3}_D$	$\mathbf{III}_D$	$\mathbf{IV}_D$	fast	1.12 ± 0.14
			slow	10.6 ± 2.1

TABLE 4: Effects of the Amino Acid Sequence in the Peptidic Guest (σ^G)

guest (I) val-leuOMe	guest (II) leu-valOMe	host (M)		$\sigma^G = (k^{XY}([M \cdot H \cdot \text{Guest (I)}]^+))/(k^{XY}([M \cdot H \cdot \text{Guest (II)}]^+))$
$\mathbf{3}_D$	$\mathbf{1}_D$	$\mathbf{I}_D$		1.66 ± 0.17
$\mathbf{3}_L$	$\mathbf{1}_L$	$\mathbf{I}_D$		0.97 ± 0.07
$\mathbf{3}_D$	$\mathbf{1}_D$	$\mathbf{I}_L$		1.04 ± 0.08
$\mathbf{3}_L$	$\mathbf{1}_L$	$\mathbf{I}_L$		1.66 ± 0.17
$\mathbf{3}_L$	$\mathbf{1}_L$	$\mathbf{II}_L$		2.17 ± 0.19
$\mathbf{3}_D$	$\mathbf{1}_D$	$\mathbf{III}_D$		1.67 ± 0.17
$\mathbf{3}_L$	$\mathbf{1}_L$	$\mathbf{III}_D$		1.43 ± 0.12
$\mathbf{3}_D$	$\mathbf{1}_D$	$\mathbf{III}_L$		1.60 ± 0.16
$\mathbf{3}_L$	$\mathbf{1}_L$	$\mathbf{III}_L$		1.41 ± 0.16
$\mathbf{3}_D$	$\mathbf{1}_D$	$\mathbf{IV}_D$	fast	0.90 ± 0.14
$\mathbf{3}_D$	$\mathbf{1}_D$	$\mathbf{IV}_D$	slow	1.66 ± 0.37
$\mathbf{3}_L$	$\mathbf{1}_L$	$\mathbf{IV}_D$	fast	0.97 ± 0.15
$\mathbf{3}_L$	$\mathbf{1}_L$	$\mathbf{IV}_D$	slow	0.84 ± 0.15
$\mathbf{3}_D$	$\mathbf{1}_D$	$\mathbf{IV}_L$	fast	0.97 ± 0.16
$\mathbf{3}_D$	$\mathbf{1}_D$	$\mathbf{IV}_L$	slow	0.88 ± 0.17
$\mathbf{3}_L$	$\mathbf{1}_L$	$\mathbf{IV}_L$	fast	1.12 ± 0.17
$\mathbf{3}_L$	$\mathbf{1}_L$	$\mathbf{IV}_L$	slow	1.62 ± 0.26

σ^G of $[M \cdot H \cdot \mathbf{1}]^+$ vs $[M \cdot H \cdot \mathbf{3}]^+$, with the guests having the same configuration, provide a measure of the effect of the amino acid sequence of the guest (Table 4). Similarly, the rate constant ratios σ^H of $[\mathbf{I} \cdot H \cdot A]^+$ vs $[\mathbf{III} \cdot H \cdot A]^+$, with the hosts having the same configuration, provide a measure of the effect of the amino acid sequence in the host pendants (Table 5).

The effects of the estereal functionalities of both the guest (ε^G) and the host pendants (ε^H) on the reaction kinetics is as large as their values diverge from unity. The same can be said as regards to the effects of the peptide sequencing in the guest (σ^G) and in the host pendants (σ^H) on the reaction kinetics.

The lack of any appreciable effects of the B configuration on the reaction 1a and 1b kinetics suggests that the B amine can displace the neutral dipeptide A from the complex without necessarily entering the chiral lower-rim cavity of the host. Since the displacement requires the direct transfer of the proton from the guest to the amine B, the lack of B configurational effects

TABLE 5: Effects of the Amino Acid Sequence in the Host Pendants (σ^H)

guest A	host (I) pendant **W** = -val-leuOMe	host (II) pendant **W** = -leu-valOMe	$\sigma^H = (k^{XY}([\text{Host (I)}\cdot H\cdot A\ ]^+))/(k^{XY}([\text{Host (II)}\cdot H\cdot A\ ]^+))$
$\mathbf{1}_D$	$\mathbf{III}_D$	$\mathbf{I}_D$	0.52 ± 0.06
$\mathbf{1}_L$	$\mathbf{III}_D$	$\mathbf{I}_D$	0.74 ± 0.05
$\mathbf{1}_D$	$\mathbf{III}_L$	$\mathbf{I}_L$	0.65 ± 0.06
$\mathbf{1}_L$	$\mathbf{III}_L$	$\mathbf{I}_L$	0.49 ± 0.05
$\mathbf{2}_L$	$\mathbf{III}_D$	$\mathbf{I}_D$	0.76 ± 0.07
$\mathbf{2}_L$	$\mathbf{III}_L$	$\mathbf{I}_L$	0.36 ± 0.05
$\mathbf{3}_D$	$\mathbf{III}_D$	$\mathbf{I}_D$	0.52 ± 0.09
$\mathbf{3}_L$	$\mathbf{III}_D$	$\mathbf{I}_D$	1.09 ± 0.10
$\mathbf{3}_D$	$\mathbf{III}_L$	$\mathbf{I}_L$	1.00 ± 0.08
$\mathbf{3}_L$	$\mathbf{III}_L$	$\mathbf{I}_L$	0.41 ± 0.04

points to a most favored $[M\cdot H\cdot A]^+$ structure wherein the A guest is essentially located on the external surface of the host between two adjacent pendants. This structural arrangement is fully consistent with independent NMR 1D ROESY evidence.[14]

Reaction 1a and 1b kinetics is rather sensitive to the nature of the estereal function of the dipeptidic guest A, as testified by the $\varepsilon^G > 1$ factors of Table 2 ($1.21 \pm 0.13 \le \varepsilon^G \le 2.09 \pm 0.28$). In contrast, the $\varepsilon^H \approx 1$ factors in the upper part of Table 3 ($\varepsilon^H = 0.88 \pm 0.07$, 0.85 ± 0.09) point to the reaction 1a and 1b kinetics as rather insensitive to the specific estereal functions of the M pendants, whether COOMe or COOEt. These findings, combined with the lack of any appreciable effects of the B configuration on the reaction kinetics, point to the A guest placed outside the host cavity in $[M\cdot H\cdot A]^+$ (M = **I**−**III**) and interacting with two host pendants in such a way that its most basic NH_2 site[16] is proton-bonded to the −CO−NH− group of a pendant nearest the aromatic rim, while the estereal tail of A is hydrogen-bonded to another adjacent pendant. This arrangement leaves the estereal tail of the M pendants free from any significant involvement in the noncovalent bonding with the A guest. This hypothesis also conforms to the NMR 1D ROESY evidence on the same neutral systems.[14] A similar arrangement can be assigned to the $[\mathbf{IV}\cdot H\cdot A]^+_{fast}$ (A = **1**, **3**) structures as well on the grounds of their limited ε^H ratios relative to the $[\mathbf{III}\cdot H\cdot A]^+$ analogues ($0.6 < \varepsilon^H < 4.0$; Table 3). In contrast, the presence of the COOH function in the host pendants of $[\mathbf{IV}\cdot H\cdot A]^+_{slow}$ (A = **1**; **3**) strongly depletes their reaction efficiencies relative to those of $[\mathbf{III}\cdot H\cdot A]^+$ ($8.6 < \varepsilon^H < 71.7$; Table 3). These findings point to large differences in the structural features of $[\mathbf{IV}\cdot H\cdot \mathbf{A}]^+_{slow}$ relative to those of both $[M\cdot H\cdot A]^+$ (M = **I**−**III**) and $[\mathbf{IV}\cdot H\cdot \mathbf{A}]^+_{fast}$, favored by the tendency of the COOH tail of **IV** pendants to act as a proton-bonding "hook" for the dipeptidic guest.

These diverse structural features are reflected in the different γ enantioselectivity factors of Figure 3 ($[M\cdot H\cdot A]^+$ (M = **I**−**III**): $\gamma < 1$; $[\mathbf{IV}\cdot H\cdot A]^+_{slow}$: $\gamma \ge 1$). Following the NMR indications,[14] the $\gamma < 1$ factors measured with $[M\cdot H\cdot A]^+$ (M = **I**−**III**) can be rationalized in terms of the greater stability of the homochiral $[M\cdot H\cdot A]^+$ complexes relative to the heterochiral ones. Reactions 1a and 1b exhibit the highest enantioselectivity with the diastereomeric $[\mathbf{III}\cdot H\cdot A]^+$ (A = **1**, **3**) complexes ($0.21 \pm 0.02 \le \gamma \le 0.36 \pm 0.03$). A slightly lower selectivity is observed with the diastereomeric $[\mathbf{I}\cdot H\cdot \mathbf{1}]^+$ ($\gamma = 0.44 \pm 0.04$, 0.31 ± 0.06) and $[\mathbf{II}_L\cdot H\cdot \mathbf{1}]^+$ ($\gamma = 0.32 \pm 0.03$) complexes. The lowest selectivity is observed with their $[\mathbf{I}\cdot H\cdot \mathbf{3}]^+$ analogues ($\gamma = 0.75 \pm 0.03$, 0.50 ± 0.02).

Comparison of the γ factors of Figure 3 with the σ^G and σ^H ones of Tables 4 and 5 reveals that, although the $[\mathbf{III}\cdot H\cdot A]^+$ (A = **1**, **3**) complexes display a similar enantioselectivity, the $[\mathbf{III}\cdot H\cdot \mathbf{3}]^+$ complexes are more reactive than the $[\mathbf{III}\cdot H\cdot \mathbf{1}]^+$ ones ($1.41 \pm 0.16 \le \sigma^G \le 1.67 \pm 0.17$) (Table 4). In the same way, the homochiral $[\mathbf{I}\cdot H\cdot \mathbf{3}]^+$ complexes appear to be more reactive than the $[\mathbf{I}\cdot H\cdot \mathbf{1}]^+$ ones ($\sigma^G = 1.66 \pm 0.17$), whereas their heterochiral counterparts are equally reactive ($\sigma^G = 0.97 \pm 0.07$, 1.04 ± 0.08). A similar trend is observed for the $[\mathbf{IV}\cdot H\cdot A]^+_{slow}$ complexes, whereas their fast isomers exhibit an equal reaction efficiency ($0.90 \pm 0.14 \le \sigma^G \le 1.12 \pm 0.17$) (Table 4). Given the comparable basicity of **1**−**3**,[16,17] these trends can only be ascribed to structural and steric effects. The differences in the σ^G factors between $[\mathbf{IV}\cdot H\cdot A]^+_{slow}$ and $[M\cdot H\cdot A]^+$ (M = **I**−**III**) may reflect the different orientation of the A guest relative to the M pendants. The differences in the σ^G factors between the homochiral and the heterochiral complexes with **I**−**III** can be only ascribed to different steric effects between the isopropyl and isobutyl groups of the guest and those of the host pendants. Both M/A steric and orientation factors may affect, on one side, the thermodynamic stability of the complexes and, on the other, the access of the base B to the protonated −CO−NH− group of the pendant holding the NH_2 head of the dipeptide.[16] This view is further corroborated by the $\sigma^H < 1$ measured with all $[M\cdot H\cdot \mathbf{1}]^+$ complexes and with only the homochiral $[M\cdot H\cdot \mathbf{3}]^+$ ones (Table 5).

On the ground of the present kinetic and previous NMR evidence, it is concluded that (a) the guests A are predominantly located in a position external to the peptidoresorc[4]arene cavity, (b) the guests A establish noncovalent interactions with the **I**−**III** pendants. Their NH_2 head is proton-bonded to the pendant amido group closer to the aromatic rim of the host, while their estereal tail is H-bonded to the polar groups of the adjacent pendant, (c) with this arrangement, both the reaction efficiency and enantioselectivity of the $[M\cdot H\cdot A]^+$ (M = **I**−**III**) complexes depend exclusively on the relative configuration of the chiral centers of the M/A pair, and (d) the presence of the COOH tail in the **IV** pendants deeply modifies the network of noncovalent interactions between the host and the estereal A guests. Thus, formation of a complex with a structure similar to those of $[M\cdot H\cdot A]^+$ (M = **I**−**III**) (the fast isomer) is accompanied by a more stable isomer wherein the guest is bound to the COOH tail of the host pendants (the slow isomer). The relative orientation and configuration of the A guest and the M pendants may affect the relative stability of the $[M\cdot H\cdot A]^+$ complexes as well as the access of the base B to the reaction center.

Experimental Section

Materials. Enantiomerically pure A = **1**−**3** and M = **I**−**IV**, in their flattened-cone conformation, were synthesized and purified according to established procedures.[16] (*R*)-(−)-2-Butylamine (B) was purchased from a commercial source and used without further purification. The amine was degassed in the vacuum manifold with several freeze−thaw cycles before the use.

FT-ICR-MS Experiments. The experiments were carried out with an APEX III (7T Magnet) FT-ICR-MS equipped with an Apollo ESI source (Bruker Daltonik GmbH, Bremen). Stock H_2O/CH_3OH = 1:3 solutions of M = **I**−**IV** (1×10^{-5} M), containing a 5-fold excess of A = **1**−**3** were electrosprayed through a heated capillary ($T = 50$ °C) into the external source of the FT-ICR mass spectrometer. The resulting ions were transferred into the resonance cell by a system of potentials and lenses and quenched by collisions with argon pulsed into the cell through a magnetic valve. ESI of M/A solutions leads to the formation of abundant signals, corresponding to the natural isotopomers of the proton-bound complex $[M\cdot H\cdot A]^+$, which were monitored and isolated by broadband ejection of the accompanying ions. The isolated $[M\cdot H\cdot A]^+$ complex was

allowed to react with the chiral amine B present in the cell at a fixed concentration whose values range from 1.0×10^9 to 3.5×10^9 molecules cm^{-3} depending upon its reactivity.

Acknowledgment. Work supported by the Ministero dell'Istruzione dell'Università e della Ricerca (MIUR). Financial support by Università "Sapienza", Roma, Italy (Funds for selected research topics 2008−2010), FIRST grant no. RBIP067F9E, FIRB grant no. RBPR05NWWC_006, and PRIN grant no. 2007H9S8SW_002 are acknowledged. The partial support from the Istituto Pasteur-Fondazione Cenci Bolognetti, "Sapienza" Università di Roma, Italy, is also acknowledged. J.M. and M.C.L. also gratefully acknowledge financial support by the Deutsche Forschungsgemeinschaft (SFB 613).

Supporting Information Available: 3D-picture of a N-linked peptidoresorc[4]arene host (**III**). This material is available free of charge via the Internet at http://pubs.acs.org.

References and Notes

(1) Schneider, H. *Angew. Chem., Int. Ed. Engl.* **1991**, *30*, 1417.

(2) *Chemistry: A Chemical Approach to Enzyme Action*, 3rd ed.; Springer-Verlag: New York, 1966; p 252.

(3) Davis, A. P.; Wareham, R. S. *Angew. Chem., Int. Ed. Engl.* **1999**, *38*, 2978.

(4) Motherwell, W. B.; Bingham, M. J.; Six, Y. *Tetrahedron* **2001**, *57*, 4663.

(5) Hollfelder, F.; Kirby, A. J.; Tawfik, D. S. *Nature* **1996**, *383*, 60.

(6) For recent reviews on gas-phase enantio- and diastereoselectivity, see: (a) Speranza, M. *Chirality* **2009**, *21*, 69. (b) Schug, K. A.; Lindner, W. *J. Sep. Sci.* **2005**, *28*, 1932. (c) Speranza, M. *Int. J. Mass Spectrom.* **2004**, *232*, 277. (d) Speranza, M. *Adv. Phys. Org. Chem.* **2004**, *39*, 147. (e) Tao, W. A.; Cooks, R. G. *Anal. Chem.* **2003**, *75*, 25A. (f) Lebrilla, C. B. *Acc. Chem. Res.* **2001**, *34*, 653. (g) Dearden, D. V.; Liang, Y.; Nicoll, J. B.; Kellersberger, K. A. *J. Mass Spectrom.* **2001**, *36*, 989. (h) Filippi, A.; Giardini, A.; Piccirillo, S.; Speranza, M. *Int. J. Mass Spectrom.* **2000**, *198*, 137. (i) Schalley, C. A. *Int. J. Mass Spectrom.* **2000**, *194*, 11. (j) Sawada, M. *Mass Spectrom. Rev.* **1997**, *16*, 73. (k) Sawada, M. In *Biological Mass Spectrometry: Present and Future*; Matsuo, T., Caprioli, R. M., Gross, M. L., Seyama, T., Eds.; Wiley: New York, 1994. (l) Splitter, J. S.; Tureček, F. *Applications of Mass Spectrometry to Organic Stereochemistry*, VCH Publishers, New York, 1994.

(7) (a) Gutsche, C. D. *Calixarenes Revisited*; The Royal Society of Chemistry: Cambridge, U.K., 1998; (b) Gutsche, C. D. *Calixarenes 2001*; Asfari, Z., Böhmer, V., Harrowfield, J., Vicens J., Eds.; Kluwer Academic: Dordrecht, The Netherlands, 2001.

(8) (a) Starnes, S. D.; Rudkevich, D. M.; Rebek, J. *J. Am. Chem. Soc.* **2001**, *123*, 4659. (b) Lücking, U.; Tucci, F. C.; Rudkevich, D. M.; Rebek, J. *J. Am. Chem. Soc.* **2000**, *122*, 8880. (c) Rudkevich, D. M.; Rebek, J. *Eur. J. Org. Chem.* **1999**, 1991. (d) Rudkevich, D. M. *Bull. Chem. Soc. Jpn.* **2002**, *75*, 393.

(9) Cram, D. J.; Cram, J. M. *Container Molecules and their Guests*, The Royal Society of Chemistry: Cambridge, 1994.

(10) (a) Heinz, T.; Rudkevich, D. M.; Rebek, J. *Nature* **1998**, *394*, 764. (b) Rudkevich, D. M. in: Calixarenes 2001; Asfari Z., Böhmer V., Harrowfield J., Vicens J. Eds.; Kluwer: Dordrecht The Netherlands, 2001; p 155; (c) Hof, F.; Craig, S. L.; Nuckolls, C.; Rebek, J. *Angew. Chem., Int. Ed.* **2002**, *41*, 1488.

(11) Botta, B.; Delle Monache, G.; Salvatore, P.; Gasparrini, F.; Villani, C.; Botta, M.; Corelli, F.; Tafi, A.; Gacs-Baitz, E.; Santini, A.; Carvalho, C. F.; Misiti, D. *J. Org. Chem.* **1997**, *62*, 932.

(12) (a) Botta, B.; Botta, M.; Filippi, A.; Tafi, A.; Delle Monache, G.; Speranza, M. *J. Am. Chem. Soc.* **2002**, *124*, 7658. (b) Tafi, A.; Botta, B.; Botta, M.; Delle Monache, G.; Filippi, A.; Speranza, M. *Chem.—Eur. J.* **2004**, *10*, 4126. (c) Botta, B.; Subissati, D.; Tafi, A.; Delle Monache, G.; Filippi, A.; Speranza, M. *Angew. Chem. Int. Ed.* **2004**, *43*, 4767. (d) Botta, B.; Caporuscio, F.; Subissati, D.; Tafi, A.; Botta, M.; Filippi, A.; Speranza, M. *Angew. Chem. Int. Ed.* **2006**, *45*, 2717. (e) Botta, B.; Caporuscio, F.; D'Acquarica, I.; Delle Monache, G.; Subissati, D.; Tafi, A.; Botta, M.; Filippi, A.; Speranza, M. *Chem.—Eur. J.* **2006**, *12*, 8096.

(13) Botta, B.; Delle Monache, G.; Fraschetti, C.; Nevola, L.; Subissati, D.; Speranza, M. *Int. J. Mass Spectrom.* **2007**, *267*, 24.

(14) Botta, B.; D'Acquarica, I.; Delle Monache, G.; Subissati, D.; Uccello-Barretta, G.; Mastrini, M.; Nazzi, S.; Speranza, M. *J. Org. Chem.* **2007**, *72*, 9283.

(15) Su, T. *J. Chem. Phys.* **1988**, *88*, 4102–5355.

(16) (a) Nold, M. J.; Cerda, B. A.; Wesdemiotis, C. *J. Am. Soc. Mass Spectrom.* **1999**, *10*, 1. (b) Pingitore, F.; Polce, M. J.; Wong, P.; Wesdemiotis, C. *J. Am. Soc. Mass Spectrom.* **2004**, *15*, 1025.

(17) Val-leu and leu-val dipetides exhibit the same gas-phase basicity (GB = 211.2 kcal mol^{-1}; http://webbook.nist.gov). It is plausible that their 1−3 esters display the same GB as well.

JP904374H